THE ASTROPHYSICAL JOURNAL, 462:114–124, 1996 May 1

BAR DISSOLUTION AND BULGE FORMATION: AN EXAMPLE OF SECULAR DYNAMICAL EVOLUTION IN GALAXIES

COLIN A. NORMAN
Department of Physics and Astronomy, Johns Hopkins University, Baltimore, MD 21218; and Space Telescope Science Institute
J. A. SELLWOOD
Department of Physics and Astronomy, Rutgers University, P.O. Box 849, Piscataway, NJ 08855-0849
AND
HASHIMA HASAN[1]
Space Telescope Science Institute, 3700 San Martin Drive, Baltimore, MD 21218
Received 1994 June 16; accepted 1995 November 8

ABSTRACT

We discuss secular changes in the stellar distribution in a barred disk galaxy that may result from substantial inflows of gas. We present two- and three-dimensional N-body simulations of a disk galaxy in which we mimic the build up of gas at the center after a strong bar has formed. We show that the bar dissolves quickly and almost completely if the core mass exceeds $\sim 5\%$ of the combined disk and bulge mass of the galaxy model we adopt. While this result agrees with our previous single-particle orbit calculations, the exact fraction for bar dissolution may well depend on the galaxy model adopted and requires further study. Bar formation and subsequent thickening and dissolution creates an additional bulgelike stellar component from the central part of the disk. We build up the central concentration gradually, but the bar dissolves abruptly once the sustaining orbits aligned with the bar become stochastic. We discuss the predictions of such a model, including the point that barred Sc galaxies with sufficient central mass concentrations should be building bulges now. We emphasize that bulges can originate from a number of different mechanisms and discuss current evidence for bulge building and bar dissolution at both high and low redshift. It is possible that bar formation, dissolution, and bulge building may even be a recurrent process.

Subject headings: celestial mechanics, stellar dynamics — galaxies: evolution — galaxies: kinematics and dynamics — galaxies: nuclei — galaxies: structure

1. INTRODUCTION

Substantial gas inflows in barred galaxies have been studied principally because they may offer a mechanism for fueling an AGN or producing a central starburst (cf. Norman 1987, 1988a, b; Shlosman, Frank, & Begelman 1989; Hernquist 1988; Phinney 1994). Our focus in this paper, however, is on the dynamical consequences of the mass inflow for the bar and bulge of the galaxy, which are independent of the precise fate of the gas.

Our studies of the single-particle dynamics in a rotating barred potential with a central mass concentration (Hasan & Norman 1990; Hasan, Pfenniger, & Norman 1993a) suggested that the sustaining orbits of the bar disappeared for rather modest central mass concentrations. Indications that such mass concentrations do exist in a sample of nearby galaxies have been presented by Richstone (1993) and Kormendy et al. (1993), on the basis of *Hubble Space Telescope* observations. These observations and recent theoretical work stimulated us to attempt N-body simulations to test whether a self-consistent bar that was free to adjust to a growing central mass concentration would in fact be dissolved by a relatively small nuclear mass. If so, this would require a major revision to our view of the secular evolution of disk galaxies.

Bar dissolution has already been discussed by a number of authors; e.g., Kormendy (1982) suggested bars might dissolve into lenses. Friedli & Pfenniger (1991) and Friedli & Benz (1993) have included dissipative components in their barred galaxy simulations and found that shocks in the bar drive mass inward toward the center until the bar is destroyed.

In earlier work we had found evidence of this type of symmetry breaking effect of a central black hole or mass concentration on the structure of a nonrotating triaxial elliptical galaxy (Norman, May, & van Albada 1985). The difficulty with those pioneering N-body calculations was that it was hard to distinguish real secular evolution from the effects of N-body noise. In a renewed attack on this secular evolution problem, we present higher quality simulations that make it clear that even a self-consistent bar can be dissolved quite suddenly by a growing central mass. The suddenness of the changes we report make it clear that they do not simply result from N-body noise. Our aim is to determine what central mass is needed to destroy the bar and to achieve a deeper understanding of the bar destruction process.

Within the past year, a number of the ideas contained in this paper have become rather fashionable, and we wish to add some balance to the current discussion. There are a number of mechanisms that can produce bulges from disks such as dissipative collapse, stellar merging, starburst systems, disk heating, etc. The detailed calculations described here show the physics of only one such mechanism. It is also clear that old bulges formed in dissipative collapse must exist as discussed below (Fisher, Franx, & Illingworth 1995). In fact, there is mounting observational evidence that there are many ways to make and evolve bulges, and we expect that many of them actually happen

[1] Present address: Astrophysics Division, NASA Headquarters, Washington, DC 20546.

and that also many provide some form of Hubble sequence evolution.

We first discuss the most recent observational and theoretical developments. New observational evidence for secular evolution including bulge building from disks is as follows:

1. Peletier (1995) has obtained *K*-band images of spiral galaxies showing that the bulge and the disk form a smooth morphological unit. Combining the *K*-band with *B*-band images, he infers using population synthesis arguments that the bulge and the disk are both of a similar population that formed less than a few billion years of each other. Andredakis, Peletier, & Balcells (1995) argue from luminosity profiles that the formation of or interaction with the disk has affected the density distribution of the bulge.

2. De Jong (1995, chap. 2, Fig. 2) shows that (*a*) lower luminosity bulges have shallower (i.e., less centrally peaked) surface brightness profiles. (*b*) The scale length of the bulge is ~ 0.1 times the scale length of the disk and that this relation is independent of Hubble type! (§ 5.3).

3. The analysis of *COBE* data on the Galactic bulge by Dwek et al. (1995) shows that for the model, E3 (Kent, Dame, & Fazio 1991), which is indistinguishable from their most favored model, G2, the disk and the boxy bulge smoothly merge into one another. Here the bulge scale height is of order 250 pc and in model G2 it is 450 pc, roughly twice the disk scale height.

4. From the spectacular Medium Deep Survey (MDS) data (Ratnatunga et al. 1995; R. Griffiths, private communication 1995) it seems that in the *I* band, brighter than $I \leq 21$, the ratio of the half-light radius of the bulge to the half-light radius of the disk is ~ 0.4 with a large spread. The redshifts of these galaxies are presumed to be of order 0.3–0.5. A detailed comparison with a local sample has yet to be undertaken.

5. Many galaxies from the CFRS survey observed with *HST* have blue nucleated concentrations, and there is approximately a magnitude increase in the mean central surface brightness of the disks at higher redshift (Schade et al. 1995).

Arguments against secular-evolution driven bulge building and for old bulges come from the following:

1. Fisher et al. (1995) have obtained Mg II gradient data for nine edge-on S0 galaxies along both the major and minor axes. They find gradients to large radii along the minor axis while along the major axis the slope of the Mg II index flattens into the disk. The much lower metallicity of the stars far from the plane would seem to indicate that at least part of the bulge is older than the disk.

2. The fundamental plane for bulges seems not to have altered much in clusters from a redshift of order a half until now (Franx 1995).

3. For the Galaxy, Gilmore (1995) notes that the cumulative angular momentum distribution of the bulge is very different from that of the disk, a fact that any bulge formation scenario must account for. More compellingly, Wyse & Gilmore (1995) argue that the metallicities of bulge stars extend much further down than those of the disk. Gilmore's conclusion that we cannot get the bulge of the Galaxy from the disk may be overstated, but the low-metallicity stars do present a problem, as for point 1.

4. Ortolani et al. (1995) claim that the bulge population in Baade's window is well matched by the luminosity function of stars in 47 Tuc, which they interpret as evidence for an old bulge. This is in striking contrast to the arguments of Rich (1992) and McWilliam & Rich (1994), who argue strongly for a young population in the same bulge stars.

5. Old populations are seen at high redshift in both ellipticals and S0 bulges (Dickinson 1995; Schade et al. 1995).

Theoretical arguments for secular evolution come from the following:

1. Friedli & Benz (1995) have continued their examination of the secular evolution of barred galaxies, including realistic models of gas flow and star formation.

2. Barnes & Hernquist (1995) have shown that when enough cool gas is accumulated at the center of a triaxial galaxy, then the entire galaxy can become axisymmetric. The physical basis for this effect was discussed by Norman (1984), Norman et al. (1985), and Gerhard & Binney (1985) for nonrotating galaxies. In essence, stars moving on box orbits in a slowly rotating triaxial stellar system will inevitably pass close to the central symmetric mass, when the orbit shape will be changed. Destruction of box orbits by the central mass makes it impossible for the mass distribution to remain elongated, and the galaxy will become axisymmetric.

3. Merritt & Fridman (1995) have shown that chaotic orbits exist in realistic triaxial potentials in analogy to the three-dimensional work done by Hasan et al. (1993a). They point out that such orbits may contribute to a slow secular evolution of galaxies.

On the other hand, Miller (1995) emphasizes that bars are rugged, and the fact that they are present in nearly all galaxies in *K*-band images is an indication of how long-lived they are. He notes that secular evolution is likely, but it takes more than might be expected to destroy a bar.

We are at a wonderful time in our understanding of bulge formation with an increasing availability of detailed data both at high and low redshift and the capability of more accurate simulations and in-depth understanding of the physical processes that drive secular evolution. What must be done on the theoretical side is to very clearly identify the physical processes underlying different ways to make bulges. In this paper we examine one such process for high-quality simulations of the central mass concentration-bar dissolution model. We study here secular dynamical evolution processes that are stellar dynamically driven, but we suspect that most of the secular evolution processes that drive the evolution of galaxies have as their ultimate origin the dissipative gaseous processes, which, although acting slowly, can act to produce profound changes over a Hubble time.

2. BAR DISSOLUTION IN TWO DIMENSIONS

2.1. *Model*

Simulations of a rotating barred galaxy in which a dense central mass concentration develops are especially challenging because of the large range of timescales between the center and periphery. We therefore address the problem first with simplified simulations in which particles are confined to a plane and later present a few fully three-dimensional results.

Our models have 75% of their total mass in an active disk and the remainder in the bulge and core components. The

three models we report in detail here differ by the mass in the core components that varies by 0%, 3%, and 7% of the total galactic mass, M.

The disk in our models has the Kuz'min-Toomre (K-T) surface density distribution

$$\Sigma(R) = \frac{Mq}{2\pi a^2}\left(1 + \frac{R^2}{a^2}\right)^{-3/2}, \quad (1)$$

where R is the distance from the center and a the length scale. The disk fraction $q = 0.75$, so that Mq is the mass of the disk extending to infinity. We select initial positions for the particles randomly from this disk density distribution truncated at $R = 6a$.

The remaining 25% of the mass is contained in the bulge and core components, the potential of which is modeled by two concentric, unresponsive, Plummer spheres

$$\Phi_{\rm ext}(r, t) = -\frac{GM_b}{(r^2 + A_b^2)^{1/2}} - \frac{GM_c}{[r^2 + A_c^2(t)]^{1/2}}, \quad (2)$$

where $M_{b(c)}$ is the mass and $A_{b(c)}$ the radius of the bulge (core), and $M_b + M_c = (1 - q)M$. Initially, both Plummer spheres have the same size with $A_b = A_c(0) = a/2$; we reduce the scale size of the core A_c over a limited period only, choosing a cubic time dependence to avoid sudden changes in slope.

The disk particles are given initial random velocities about circular orbits so as to make Q, Toomre's local stability parameter, equal to unity in the combined potential of the disk and bulge components. We then adjust the orbital velocities according to the Jeans equations to establish approximate radial balance.

The force field at distance d from a unit mass particle is derived from the standard "softened" potential $\Phi(d) = -G(d^2 + \epsilon^2)^{-1/2}$, where the softening length, ϵ, is a constant. We tabulate the field of the particles on a two-dimensional polar grid (Sellwood 1981) and compute their motion using longer time steps in two outer zones (Sellwood 1985) to improve efficiency. The grid has 110 radial and 128 azimuthal nodes, $\epsilon = 0.05a$, we employ 50,000 particles, and the time step in the inner zone is 0.004. We adopt a and M as our units of length and mass, respectively; our time units are therefore dynamical times $(a^3/GM)^{1/2}$.

We allow the model to evolve with unchanging bulge components until a steadily rotating bar has formed and then gradually reduce the scale radius of one Plummer sphere by a factor of 50 over about four bar tumbling periods ($t = 100$ to $t = 150$). We then continue the evolution with no further changes to the rigid components. The contraction procedure is intended to mimic the radial inflow of gas driven by the bar; it does not add any mass to the system and therefore has little effect on the rotational balance at large radii. We experiment with various fractions of the total mass in the part that forms the central core.

At intervals, we quantify nonaxisymmetric features in the particle distribution by forming the summation (Sellwood & Athanassoula 1986)

$$A(m, \gamma, t) = \frac{1}{N}\sum_{j=1}^{N} \exp\left[im(\theta_j + \tan\gamma \ln R_j)\right], \quad (3)$$

where (R_j, θ_j) are the coordinates of each of the N particles in the simulation at time t. This two-dimensional Fourier transform yields the amplitudes and phases of a set of logarithmic spiral components, with γ a (constant) angle between the ridge line of the spiral component and the radius vector. The $m = 2$, $\gamma = 0$ (radial) term in this expansion provides an estimate of the bar amplitude.

2.2. *Results*

The behavior of three of our models is illustrated in Figure 1. The top row shows the long-lived bar in a model

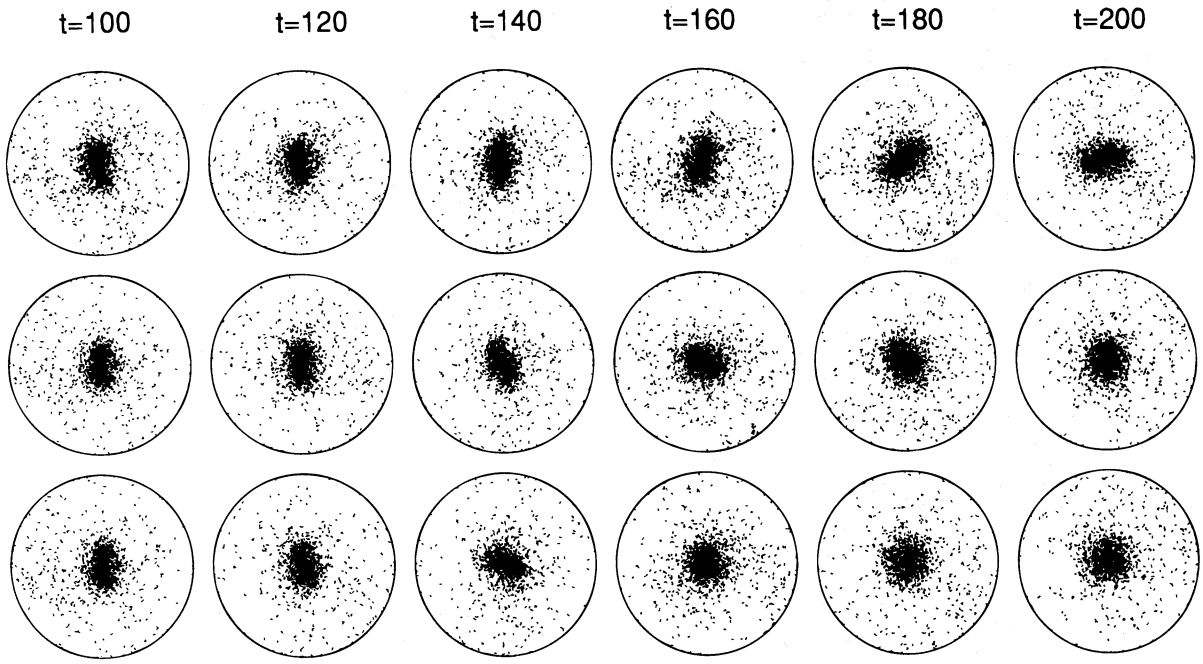

FIG. 1.—The evolution of the inner parts of three separate models from $t = 100$ to $t = 200$; the circles are drawn at $r = 5a$, which is about half the mesh radius. The top row shows the equilibrium state of the barred disk simulation when there is no central mass; the bar rotates steadily at constant amplitude. The middle row shows the evolution that results from shrinking 3% of the total mass between times $t = 100$ and $t = 150$; note that the bar is weakened but is not totally destroyed and that it remains at roughly the same low amplitude when the run is continued to time 240. The bottom row shows the evolution when 7% of the mass is shrunk, again from $t = 100$ to $t = 150$; in this case the bar is totally destroyed between times 140 and 160.

in which A_c is held fixed at its initial value so that no central mass concentration is formed; the middle row shows how the bar is affected by a central core component containing 3% of the total mass that was formed during the first half of the period illustrated; by the end of the run at $t = 240$ the bar has been significantly diminished although not completely. A 7% central mass was created in the model in the bottom row and the bar is abruptly destroyed even before the contraction of the core is complete. Other experiments (not illustrated) examined the 1% and 5% cases.

To verify that the evolution was unaffected by the rate of core contraction, we slowed it by a factor of 2 and found that the bar changed just as suddenly and at the same bulge size as for the more rapid contraction.

Figure 2 shows the variation of the amplitude of the bar ($m = 2$, $\gamma = 0$) component for the three values of the central mass = 0, 3%, and 7%. The rms amplitude of this Fourier component over the last part of the run is shown as a function of the central mass in Figure 3.

These results indicate that a central mass greater than $\sim 5\%$ of the total disk plus bulge mass will dissolve the bar, confirming the earlier single-particle orbit studies of Hasan & Norman (1990) and Hasan et al. (1993a).

2.3. *Surfaces of Section*

In order to understand the bar dissolution process, we compute surfaces of section (SOS) in a rotating time-invariant potential that represents an average of the potential in the simulations over a period of 50 dynamical times. To obtain this average, we rotated the density distribution at each time through an angle determined by the initial phase and average pattern speed during this period so as to produce a combined bar density distribution that was aligned with the x-axis. We then computed the force field and potential of the averaged density distribution. We have done this for two models: for the run without a core, we selected 51 density distributions spanning the period from $t = 100$ to $t = 150$ during which time the bar rotated steadily at approximately constant amplitude. For the model with a 3% core mass, we averaged over the period from $t = 150$ to $t = 200$, i.e., after the core shrinking was completed and the bar had adjusted to the new potential.

Figures 4 and 5 show SOSs for various values of the Jacobi constant, H (loosely referred to as the Hamiltonian), for the zero and 3% central mass models. Particles of a fixed H are confined by their energies to the region bounded by the curves in these figures, and we select the value for each SOS by the limiting distance, y_0, a particle may reach on the bar minor axis, denoting this by $H(0, y_0)$.

As usual, we integrate the equations of motion in the averaged force field and record $(y, \dot{y})$ values every time the orbit crosses the bar minor axis with $\dot{x} < 0$. The right-hand side of the plots therefore corresponds to crossings in the direct sense, while the left-hand side corresponds to retrograde crossings of the bar minor axis.

The SOSs for six Hamiltonian values are shown for the

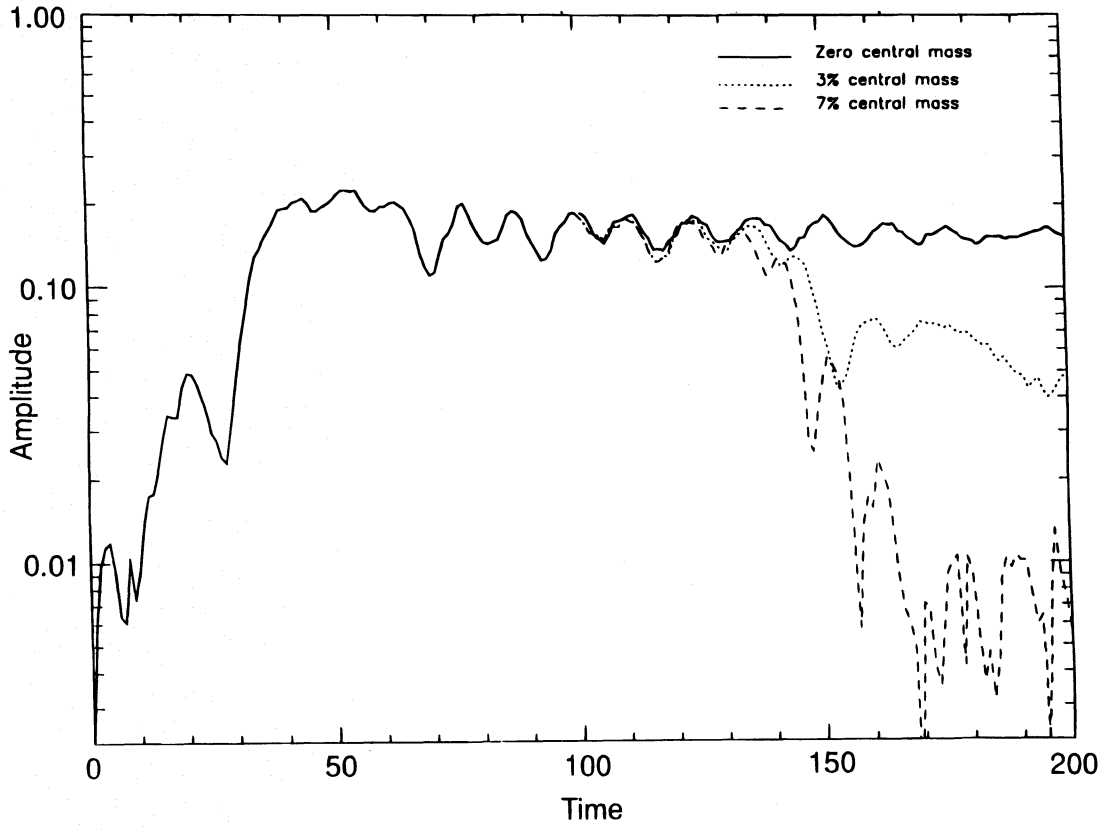

FIG. 2.—The variation of the amplitude of the $m = 2$ bar component with time for central masses of 0%, 3%, and 7%. The fluctuations in the bar amplitude for the case of no central mass are due to beats between the bar and the residual spirals in the outer disk, but no secular decay is seen. When a 3% central mass is created, the bar amplitude drops some 50% (at $t \simeq 150$) and decays only slightly more in the remainder of the simulation. A 7% central mass causes a dramatic drop in amplitude of the bar component at $t \simeq 145$, after which the amplitude is barely larger than the noise level (0.004 for 50 K particles).

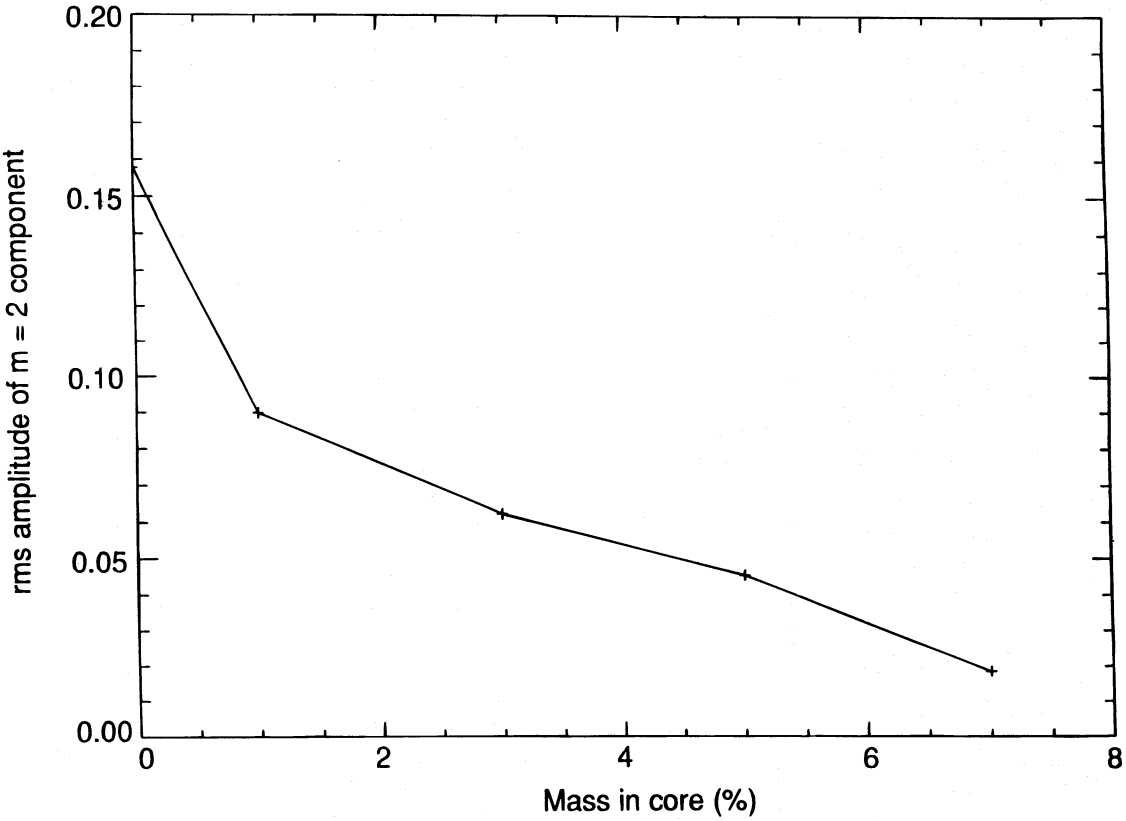

FIG. 3.—The rms amplitude of the final bar component as a function of the central mass. The final amplitude decreases continuously as the central mass concentration is increased, and the bar is effectively destroyed when the central mass is greater than ~5% the galactic mass.

model without a core in Figure 4. All show a large regular region (many nested invariant curves) around the x_1 (or B) periodic orbit family, which are generally believed to form the backbone of the bar (e.g., Sellwood & Wilkinson 1993). The extensive invariant region on the left of these plots is of little interest, since those orbits are retrograde and will not be heavily populated. It is hard to follow the invariant curves for all cases, and they sometimes give the appearance of crossing, which can happen only when, as here, the forces are not the precise derivatives of the adopted potential function.

The SOS for the 3% central mass (Fig. 5) shows that the regular region occupied by x_1 orbits decreases as we look at more tightly bound values of H until the associated invariant curves have completely dissolved for the $H(0, 0.6)$ case. New, boomerang-shaped, invariant curves associated with the perpendicular (x_2) family of orbits become very pronounced on the right-hand side of the SOS for $H(0, 0.5)$. Thus the structure of phase space in the inner part of the bar in this model with a 3% central mass concentration is unfavorable for a self-consistent bar. The bar seems able to survive in its weakened form only because phase space at higher energies contains sufficient regularity about the x_1 family.

3. THREE-DIMENSIONAL MODELS

The particles in the foregoing simulations were constrained to remain in the plane and therefore do not reveal the full fate of the model. In this section we report the evolution of similar fully three-dimensional simulations to show that the particle distribution thickens perpendicular to the plane as the bar dissolves.

3.1. *Simulations*

We use a cylindrical polar grid that is a straightforward generalization of the two-dimensional code used in § 2. The planes of grid points are spaced evenly in the z-direction. We solve separately for the three components of the gravitational force field and for the potential of the mass distribution using FFTs in the vertical and azimuthal directions and by direct convolution in the radial direction.

We integrate the motion of the particles using a standard Cartesian leap-frog scheme except that, as in two dimensions, we adopt a three-zone stepping procedure in which time steps are increased for particles progressively further from the center.

As in two dimensions, we use the particles to represent the K-T disk, which in this case has slightly less mass ($q = 0.7$). In addition to setting $Q = 1$ initially, we give the disk an initial thickness $z_0 = 0.02a$ and use the one-dimensional vertical Jeans equation to determine the vertical velocity dispersion required for equilibrium. Again the bulge and the central core are represented by rigid Plummer spheres, with $A_b = A_c(0) = 0.4a$. Time units and length scales are as defined in § 2.

Our grid has 65 radial, 80 azimuthal, and 375 vertical nodes, $\epsilon = 0.02a$, we employ 200,000 particles and the shortest time step is 0.001.

The evolution when the mass of the central component is 5% is shown in Figure 6. As usual for three-dimensional simulations (see, e.g., Combes et al. 1990), the bar thickens

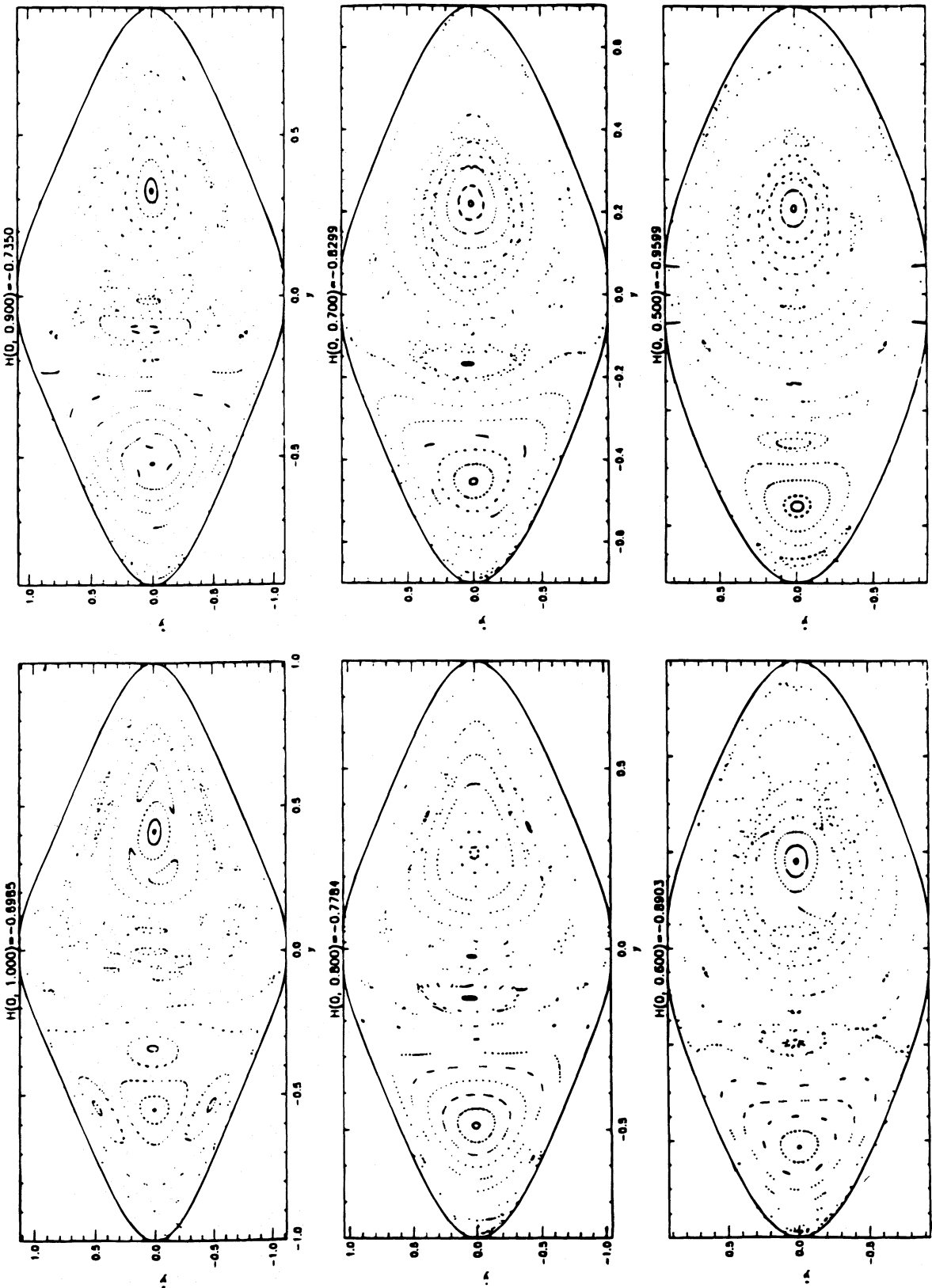

FIG. 4.—Surfaces of section for six Hamiltonian values in the zero central mass case. The Hamiltonian values selected are those for a particle momentarily at rest at six evenly spaced distances on the bar minor axis. There are large regular regions on the right-hand sides that indicate extensive trapping around the direct x_1 orbit family that supports the bar. Further details are given in § 2.3.

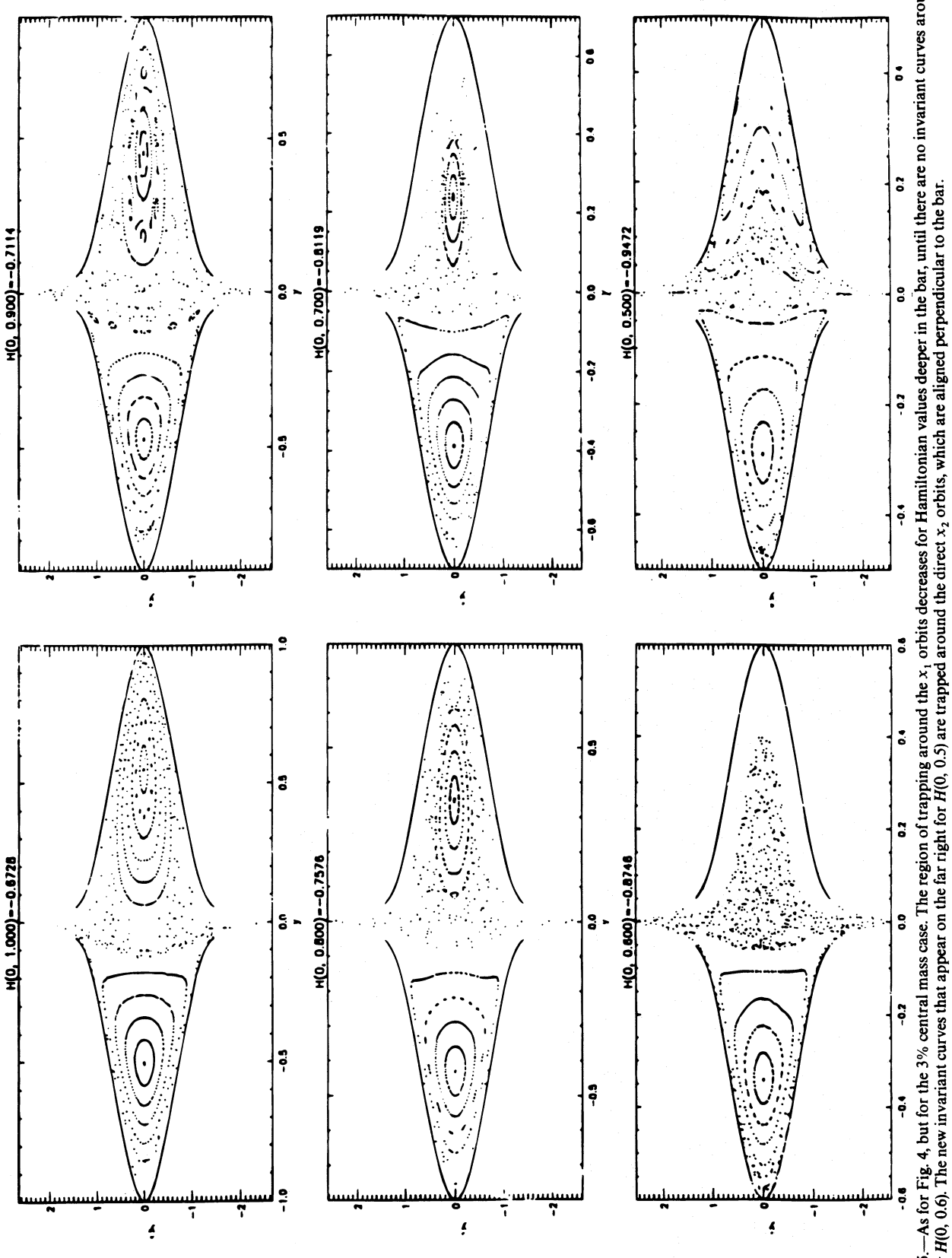

FIG. 5.—As for Fig. 4, but for the 3% central mass case. The region of trapping around the x_1 orbits decreases for Hamiltonian values deeper in the bar, until there are no invariant curves around the x_1 orbits for $H(0, 0.6)$. The new invariant curves that appear on the far right for $H(0, 0.5)$ are trapped around the direct x_2 orbits, which are aligned perpendicular to the bar.

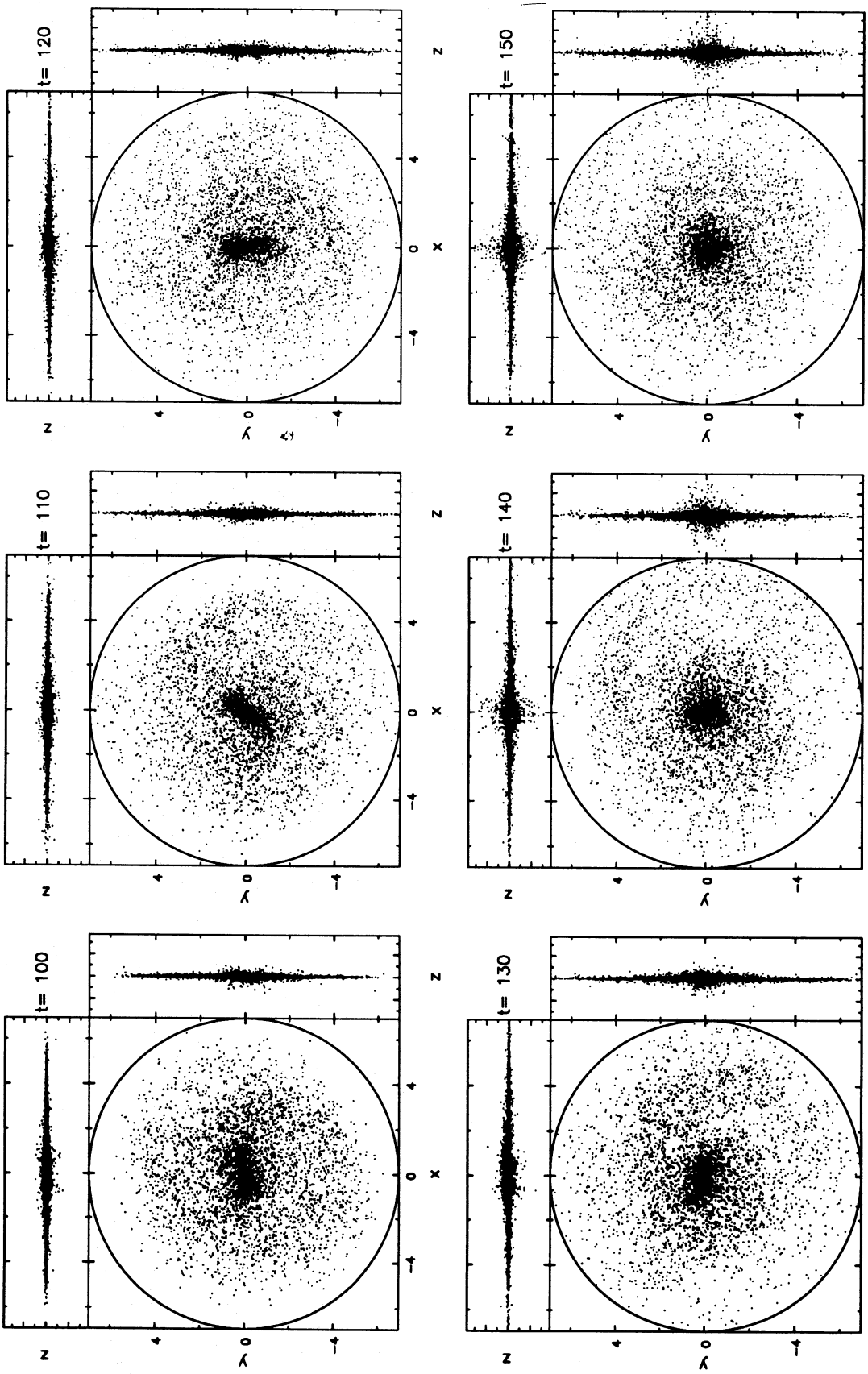

FIG. 6.—The evolution of a three-dimensional model in which a 5% central mass is grown from time 100 to time 140. The whole calculation volume is shown, but only one particle in 40 is plotted. The bar dissolves abruptly between times 130 and 140, forming a spheroidal bulgelike feature at the center.

out of the plane through a collective bending instability (Raha et al. 1991; Merritt & Sellwood 1994). The first moment, time 100, illustrates the disk component once the bar had formed, thickened, and settled. In this state, the bar has puffed up to approximately twice the scale height of the disk (cf. Dwek et al. 1995, model G2).

We gradually reduced A_c by a factor of 20 between times 100 and 140. Once again, the bar responds to this change by first increasing its pattern speed and becoming shorter before disrupting very abruptly between times 130 and 140. The bar decays just as rapidly as for the similar two-dimensional model; the amplitude of the $m = 2$, $\gamma = 0$ coefficient drops by a factor 10 in less than one bar rotation period, after which time no significant bar remains. *The new aspect in three dimensions is the quite marked thickening of the inner particle distribution as the bar dissolves; the process forms a spheroidal bulgelike distribution.*

The final face-on projected surface density distribution of the active mass in the model is shown in Figure 7, together with the density profile of the initial disk. It is not unlike a Freeman (1970) type II disk with a separate central bulge component.

As shown in Figure 8*a*, the newly formed axisymmetric bulge "component" is not boxy; in fact, it is somewhat peaky. It has approximately the mass of the dissolved bar and a scale height now considerably larger than that of the disk. Evidently there is no memory of the additional integrals of motion from the now dissolved bar. It is interesting to note that Kuijken & Merrifield (1995) find a link between box-shaped bulges and the presence of bars, as has also been concluded for the Milky Way. Our models are consistent, at least, with their finding, since there is no residual boxiness when the bar is dissolved. We note that there are galaxies with the bulge morphology seen in Figure 8*a* (K. C. Freeman, private communication). It is tempting to speculate that the morphology seen in Figure 8*a* may be the signature of a dissolved bar. In particular, we might expect the younger, more metal-rich stars that have added by our mechanish to the old, pre-existing buldge to have a spatial distribution similar to that seen in Figure 8*a*.

We emphasize at this point that the "bulge" formed from the bar particles is not the only bulge in the model; throughout the calculation we include the force from 25% of the total mass in a rigid Plummer sphere.

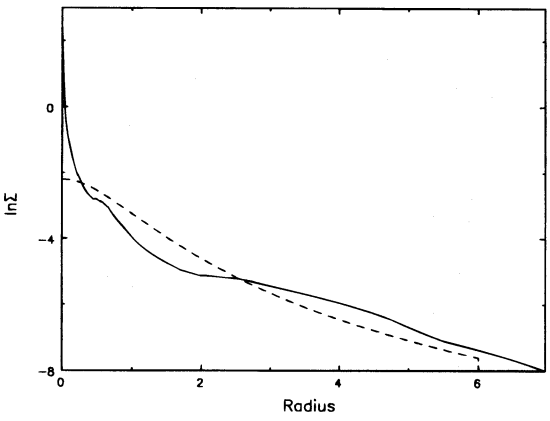

FIG. 7.—The projected surface mass distribution of the active particles in the model shown in Fig. 6 at time 150 (*solid curve*). The dashed curve shows the density profile from which the simulation began.

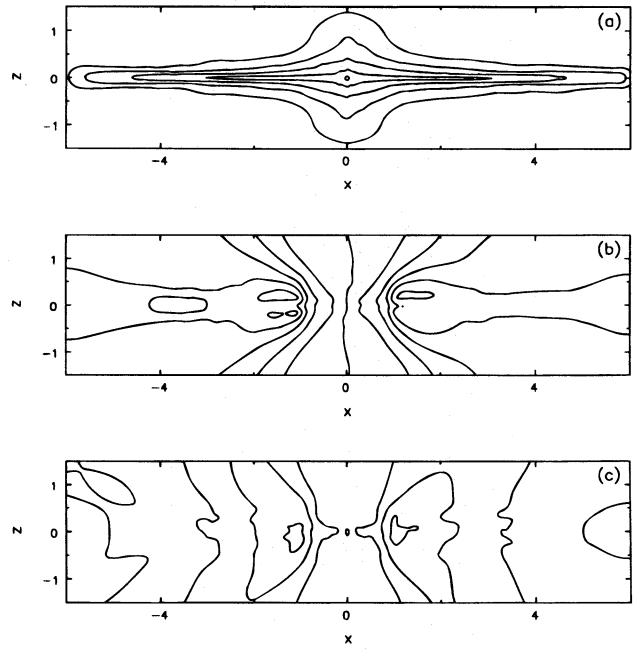

FIG. 8.—Contour plots of (*a*) the density and (*b*) the first and (*c*) the second line-of-sight velocity moments of an edge-on projection of the model shown in Fig. 6 at time 150. The smoothing kernel used for the velocity moments has twice the width of that for the density. Contours are drawn at every two magnitudes in (*a*) and are linearly spaced in (*b*) and (*c*); the zero velocity contour runs up close to the symmetry axis in (*b*) and the closed contours on either side of the center in (*c*) are local maxima in the velocity dispersion. This figure is drawn from the active particles only and ignores the rigid component.

Figures 8*b* and 8*c* show the first and second velocity moments, integrated along lines of sight through the model at this last moment. The velocity field of these particles does not have the cylindrical rotation pattern of either barred galaxy models (Combes et al. 1990; Sellwood 1993) or of the boxy bulges of real galaxies (see, e.g., Shaw, Wilkinson, & Carter 1993).

As in the two-dimensional case, the bar was weakened but not completely destroyed in other models, having 1% and 3% of mass in the core component.

3.2. *Bar Dissolution Mechanism*

The demise of the bar on the shortest possible timescale occurs because particles cease to be trapped about the main x_1 orbit family as the potential changes, as shown for two dimensions in § 2.3. Miller & Smith (1979) and Pfenniger & Friedli (1991) have shown that a boxy, or peanut shaped, bar is still supported by the x_1 orbit family, but the orbits are twisted antisymmetrically about the bar midplane to resemble figures of eight when seen from the side; that is, the parent orbit family is the antisymmetric 2:2:1 resonant family (Sellwood & Wilkinson 1993). Since these orbits are simple three-dimensional generalizations of the x_1 orbit family that sustains two-dimensional bars, we expect the essentials of phase space structure we found in § 2.3 to carry over to three-dimensional bars.

The growth of the central mass alters both the shapes of the periodic orbits and the volume of regular phase space, so that particles that had been moving on regular orbits suddenly find themselves in stochastic regions. The widespread breakdown of invariant tori in this rotating triaxial

potential leads to a brief period of chaos in which the orbits of particles are bounded only by their much rounder energy surfaces. A new equilibrium is quickly reached when the potential becomes axisymmetric, for which phase space is likely to be regular once more. This interpretation accounts both for the abrupt destruction of the bar and for the vertical thickening of the particle distribution.

A number of authors have offered a different interpretation of the bar dissolution. They suggest that particles are individually scattered from their bar-supporting orbits as they pass by the central mass, causing the bar to be eroded more gradually. This argument probably stems from those given by Norman (1984), Norman et al. (1985), and Gerhard & Binney (1985) for slowly rotating triaxial ellipsoids; many orbits in these objects are boxes, which take stars close to the center where a steep density gradient might change the orbit drastically and destroy the triaxiality. (Merritt & Fridman 1995 show that this does not, in fact, preclude triaxiality.) The main (x_1) orbit family in a rapidly rotating bar, on the other hand, are loops that always avoid the center. When we consider central masses small enough to cause only partial disruption of the bar, many particles pursue regular loop orbits determined by the combined potential of the bar and central mass. It could not therefore be argued that deflections accumulate as a star repeatedly passes the center, and the gradual erosion picture that the scattering argument conjures up is misleading. In effect, focusing on the scattering of a test particle by an isolated point mass neglects the existence of the rest of the bar.

4. DISCUSSION

These highly idealized calculations are intended to study just one aspect of the rich secular evolution of barred galaxies. The contraction of a rigid mass component is, of course, highly artificial and mimics in only an extremely loose way the actual process of gas inflow in a barred galaxy. Our aim, however, was not to strive for realism, with all the complications that implies, but to isolate and study a single aspect of the physics in clean and realizable experiments. Ambitious, but necessarily crude, simulations of fully self-consistent three-dimensional bars including dissipation have been reported by Friedli & Benz (1993, 1995) and Heller & Shloshman (1994) and appear to be in broad agreement with our results.

We have shown that building a dense concentration of mass at the center of a bar gradually reduces the volume of phase space accessible to regular, bar-supporting orbits of the x_1 family (or its generalization to three dimensions). This gradual change eventually destroys the bar quite suddenly once the mass fraction in the dense core reaches some relatively small fraction of the combined mass of the disk and bulge. In our models, the dense core mass needed to be 5% of the combined disk and bulge mass to dissolve the bar, but exact critical mass will probably depend on the properties of the galaxy and its bar and remains to be determined from more extensive calculations. Since our previous estimates of the critical mass from single-particle orbits agree well with the self-consistent calculations here, that simplified approach may well be adequate for such an exploration.

We do not argue that all bulges are formed by bar dissolution, bulge heating, and associated secular evolutionary processes, merely that such process must populate bulges with disk material. Other bulge-forming scenarios, such as enhanced star formation rates in the central part of the collapsing cloud (cf. Eggen, Lynden-Bell, & Sandage 1962; Sandage 1986) or mergers of partially formed galaxies in the early universe (e.g., Carlberg 1992), etc., may well play substantial roles also. However, our proposed mechanism naturally leads to bulges with a high degree of rotational support. Moreover, it is not essential for the bar to be destroyed in order to make a bulge—a conclusion exemplified by the strong photometric and kinematic correspondence between the Milky Way bulge and a barred galaxy model (Sellwood 1993). In the Galactic Bulge, Zhao et al. (1995) have analyzed stellar proper motions in Baade's Window and infer that the metal-rich component is rotationally supported.

Currently we do not know from either observational or theoretical studies whether this type of process actually leads to significant late time evolution along the Hubble sequence. Observations of galaxy morphology at high redshift with the *Hubble Space Telescope* will help answer this question (cf. Dressler et al. 1996; Griffiths et al. 1994; Schade et al. 1995) when the high-redshift distribution of galaxies along the Hubble sequence is compared to the normal low-redshift distribution. This is almost possible, but the sample is still too small (Schade et al. 1995). Catching a galaxy in the act of bulge formation by observing a suitable barred Sc with a sufficiently large central mass concentration and with a Population I bulge and disk kinematics may also be very productive. One fascinating area where this bar dissolution, bulge formation, and bar stabilization process is clearly seen is in the beautiful cosmical simulations of Steinmetz (1995). Owing to the overcooling effect that dominates such systems without adequate feedback, very significant amounts of gas fall into the central regions of the forming galaxies. Initially formed bars then dissolve, and the disk galaxies thenceforth evolve without bars.

The overriding motivation for the work described here is to develop an understanding of the evolutionary tracks of galaxies, driven by the slow gas dynamic and stellar dynamical processes inexorably at work in galaxies. Such a program involves not only detailed physics calculations but also most likely a reassessment of the observational data and theoretical parameter sets that most clearly describe galaxies as they evolve from high to low redshift (cf. Djorgovskii et al. 1995; Driver et al. 1995; Griffiths et al. 1994). This grand program is similar to that of computing stellar evolutionary tracks and possibly even more difficult, but it is extremely worth undertaking. Note that, as with some stellar tracks, galaxies may recurrently move from a barred to an unbarred phase and undergo recurrent and continuing bulge building as the bars dissolve. The new *HST* data from the MDS (Griffiths et al. 1994) and other deep field studies (Giavalisco et al. 1995; Dickinson et al. 1995) more or less mandates such an effort.

This work has gained much from our many conversations with George Contopoulos, Mark Dickinson, George Djorgovskii, Eli Dwek, Daniel Friedli, Ken Freeman, Marijn Franx, Richard Griffiths, Garth Illingworth, John Kormendy, Daniel Pfenniger, Mike Rich, Doug Richstone, and Mattheus Steinmetz. J. A. S. acknowledges support from NSF grant AST 93-18617 and NASA Theory grant NAG 5-2803.

REFERENCES

Andredakis, Y. C., Peletier, R. F., & Balcells, M. 1995, MNRAS, in press
Barnes, J., & Hernquist, L. 1995, in IAU Symp. 171, Evolution of Galaxies, ed. R. Bender & R. D. Davies (Dordrecht: Kluwer), in press
Carlberg, R. G. 1992, ApJ, 399, L31
Combes, F., Debasch, F., Friedli, D., & Pfenniger, D. 1990, A&A, 233, 82
de Jong, R. S. 1995, Ph.D. thesis, Univ. of Groningen
Dickinson, M. 1995, in ASP Conf. Ser., Fresh Views on Elliptical Galaxies, ed. A. Busoni, A. Renzini, & A. Serrano (San Francisco: ASP), in press
Djorgovskii, S. G., Pahre, M. A., & de Carvalho, R. R. 1995, in ASP Conf. Ser., Fresh Views on Elliptical Galaxies, ed. A. Busoni, A. Renzini, & A. Serrano (San Francisco: ASP), in press
Driver, S. P., Windhorst, R. A., Ostrander, E. J., Keel, W. C., Griffiths, R. E., & Ratnatunga, K. 1995, ApJ, 449, L23
Dressler, A., Oemler, A. Sparks, W. B., Williams, R. E., & Lucas, R. A. 1996, ApJ, submitted
Dwek, E., et al 1995, ApJ, 445, 716
Eggen, O. J., Lynden-Bell, D., & Sandage, A. 1962, ApJ, 136, 748
Fisher, D., Franx, M., & Illingworth, G. 1995, in IAU Symp. 171, Evolution of Galaxies, ed. R. Bender & R. D. Davies (Dordrecht: Kluwer), in press
Franx, M. 1995, in IAU Symp. 171, Evolution of Galaxies (Dordrecht: Kluwer), in press
Freeman, K. C. 1970, ApJ, 160, 811
Friedli, D., & Benz, W. 1993, A&A, 268, 65
———. 1995, A&A, 301, 649
Friedli, D., & Pfenniger, D. 1991, in IAU Symp. 146, Dynamics of Galaxies and Their Molecular Cloud Distributions, ed. F. Combes, & F. Casoli (Dordrecht: Reidel), 362
Giavalisco, M., Macchetto, F. D., Madau, P., & Sparks, W. B. 1995, ApJ, 441, L13
Gerhard, O. E., & Binney, J. 1985, MNRAS, 216, 467
Gilmore, G. 1995, in Proc. IAU Gen. Assembly, Stellar Populations, ed. P. C. van der Kruit & G. Gilmore (Dordrecht: Kluwer), 99
Griffiths, R. E., et al. 1994, ApJ, 435, L19
Hasan, H., & Norman, C. 1990, ApJ, 361, 69
Hasan, H., Pfenniger, D., & Norman, C. 1993a, ApJ, 409, 91
Hasan, H., Sellwood, J. A., & Norman, C. 1993b, in IAU Symp. 153, Galactic Bulges, ed. H. Dejonghe & H. Habing (Dordrecht: Kluwer), 385
Heller, C., & Shloshman, I. 1994, ApJ, 424, 84
Hernquist, L. 1988, Nature, 340, 687
Kent, S. M., Dame, T. M., & Fazio, G. 1991, ApJ, 378, 131
Kormendy, J. 1982, in Proc. Saas Fee Course, No. 12, Morphology and Dynamics of Galaxies, ed. L. Martinet & M. Mayor (Sauverny: Geneva Obs.), 113
Kormendy, J., Byun, Y., Dressler, A., Faber, S. M., Grillmair, C., Lauer, T.R., Richstone, D. O., & Tremaine, S. 1993, in Proc. ESA/OHP Workshop on Dwarf Galaxies, ed. G. Meylan (Garching: ESO), 147
Kuijken, K., & Merrifield, M. R. 1995, ApJ 443, L13
McWilliam, A., & Rich, R. M. 1994 ApJS, 91, 749
Merritt, D., & Fridman, T. 1995, preprint
Merritt, D., & Sellwood, J. A. 1994, ApJ, 425, 551
Miller, R. H. 1995, in IAU Colloq. 157, Conf. Summary, Barred Galaxies, ed. R. Buta, B. C. Elmegreen, & D. A. Crocker (Dordrecht: Kluwer), in press
Miller, R. H., & Smith, B. F. 1979, ApJ, 227, 785
Norman, C. 1984, in Proc. Moriond Conf. on The Formation and Evolution of Galaxies, ed, J. Audouze & J. Tran Thanh Van, NATO ASI Ser., Math. Phys. Sci., 117, 327
———. 1987, in Star Formation in Galaxies, ed. G. Neugebauer & N. Scoville (NASA Conf. Pub.), CP-2466. 395
———. 1988a, in Comets to Cosmology, ed. A. Lawrence (Berlin: Springer), 177
———. 1988b, in Galactic and Extragalactic Star Formation, ed. R. Pudritz & M. Fich, NATO ASI Ser. 232 (Dordrecht: Kluwer), 495
Norman, C., May, A., & van Albada, T. 1985, ApJ, 296, 20
Ortolani, S., Renzini, A., Gilmozzi, R., Marconi, G., Barbuy, B. Bica, E., & Rich, R. M. 1995, Nature, 377, 701
Peletier, R. 1995, in IAU Symp. 171, Evolution of Galaxies, ed. R. Bender & R. D. Davies (Dordrecht: Kluwer), in press
Pfenniger, D., & Friedli, D. 1991, A&A, 252, 75
Phinney, E. S. 1994 in Mass Transfer Induced Activity in Galaxies, ed. I. Shlosman (Cambridge: Cambridge Univ. Press), 1
Raha, N., Sellwood, J. A., James, R. A., & Kahn, F. D. 1991, Nature, 352, 411
Ratnatunga, K., et al. 1995, in preparation
Rich, M. 1992, in The Center, Bulge and Disk of the Milky Way, ed. L. Blitz (Dordrecht: Kluwer), 47
Richstone, D. 1993, in Proc. Texas/PASCOS '92, Relativistic Astrophysics and Particle Cosmology, ed. C. W. Akerlof & M. A. Srednicki (New York: NY Acad. of Sciences), 716
Sandage, A. 1986, ARA&A, 24, 421
Schade, D., Lilly, S. J., Crampton, D. Hammer, F. Le Fevre, O., & Tresse, L. 1995, ApJ, 451, L1
Sellwood, J. A. 1981, A&A 99, 362
———. 1985, MNRAS, 217, 127
Sellwood, J. A. 1993, in Back to the Galaxy, ed S. S. Holt & F. Verter (New York: AIP), 133
Sellwood, J. A., & Athanassoula, E. 1986, MNRAS, 221, 195
Sellwood, J. A., & Wilkinson, A. 1993, Rep. Prog. Phys., 56, 173
Shaw, M., Wilkinson, A., & Carter, D. 1993, A&A 268, 511
Shlosman, I., Frank, J., & Begelman, M. C. 1989, Nature, 338, 45
Steinmetz, M. 1995, in IAU Symp. 171, Evolution of Galaxies, ed. R. Bender & R. D. Davies (Kluwer: Dordrecht), in press
Wyse, R., & Gilmore, G. 1995, AJ, 110, 2771
Zhao, H., Rich, M., Applegate, J., & Biello, M. 1995, ApJ, submitted